Sustainable Chemical Engineering
https://ojs.wiserpub.com/index.php/SCE/

UNIVERSAL WISER PUBLISHER

Research Article

The Evaluation of Anticorrosive Behavior of Rigid Solvent Free Polyurethane Coatings

Merve Demirkurt[1*], Zeynep Yılmazer[1], Şinasi Bayata[1], Mustafa M. Demir[2]

[1]Kanat Paints & Coatings, Kemalpaşa Organized Industrial Zone, 500th Street, No. 321, Kemalpaşa, İzmir, Turkey
[2]Department of Materials Science and Engineering, İzmir Institute of Technology, Faculty of Engineering, Urla, İzmir, 35430, Turkey
E-mail: merved@kanatboya.com.tr

Received: 17 September 2025; **Revised:** 4 January 2026; **Accepted:** 4 January 2026

Graphical Abstract:

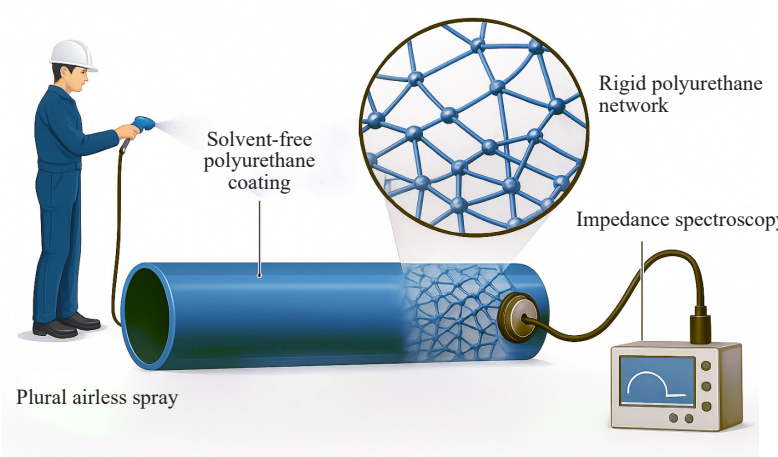

Abstract: Solvent-free rigid Polyurethane (PU) coatings are widely applied for pipeline corrosion protection due to their high-build capability, the elimination of Volatile Organic Compounds (VOCs), and suitability for structurally demanding and hygienic water-contact applications. Despite their extensive industrial use, the electrochemical degradation behavior of thick, highly resistive solvent-free PU systems-particularly under accelerated electrochemical stress-remains insufficiently clarified. Anticorrosive performance of a rigid solvent-free PU coating formulated for pipeline steel was investigated using a combined evaluation framework involving long-term Electrochemical Impedance Spectroscopy (EIS), Alternating Current-Direct Current-Alternating Current (AC-DC-AC) accelerated electrochemical cycling, and conventional durability tests, including Cathodic Disbondment (CD) and Neutral Salt Spray (NSS) exposure. Immersion EIS measurements in 5 wt% NaCl exhibited a single dominant time constant throughout the exposure period, with low-frequency impedance values exceeding 10^8 $\Omega \cdot cm^2$ and coating capacitance on the order of 10^{-9} $F \cdot cm^{-2}$. This behavior indicates a highly resistive dielectric barrier governed by restricted ionic transport within a predominantly hydrophobic polyurethane network. During AC-DC-AC cycling, the impedance response evolved from an intact-barrier

DOI: https://doi.org/10.37256/sce.7120268661

regime toward diffusion-controlled behavior, as evidenced by progressive reductions in coating resistance, changes in constant phase element parameters, and the emergence of Warburg-type diffusion features. At extended cycling times, an apparent, diffusion-limited stabilization of impedance was observed, suggesting transport limitation within confined interfacial regions rather than true barrier recovery. Notably, similar stabilization trends were detected in EIS measurements conducted after 2,500 h of NSS exposure, demonstrating a strong mechanistic correlation between accelerated electrochemical cycling and long-term environmental degradation. Cathodic disbondment testing confirmed excellent compatibility with cathodic protection systems, with disbondment values remaining well within industry acceptance limits. Overall, this work provides a mechanistically grounded electrochemical assessment of rigid solvent-free PU coatings and establishes AC-DC-AC testing as a resource-efficient and predictive approach for evaluating long-term pipeline coating performance.

***Keywords*:** solvent free coating, rigid polyurethane coating, anticorrosion, impedence spectroscopy, Alternating Current-Direct Current-Alternating Current test

1. Introduction

Pipeline systems used for potable water distribution, petrochemical transport, and buried infrastructure require protective coatings capable of providing long-term resistance against moisture ingress, ionic transport, and electrochemical degradation under complex service conditions. Among the available coating technologies, solvent-free rigid Polyurethane (PU) systems have gained increasing industrial adoption due to their high-build capability, excellent mechanical integrity, strong adhesion to steel substrates, and complete elimination of Volatile Organic Compounds (VOCs). These characteristics make them particularly attractive for environmentally regulated applications and hygienic water-contact systems.[1-3]

The barrier performance of solvent-free rigid polyurethane coatings is primarily governed by the hydrophobic nature of the polymer chains, which limits water affinity and suppresses continuous ionic pathways within the coating matrix. Network rigidity and crosslink density contribute secondarily by restricting free volume and segmental mobility, thereby reducing diffusive transport rates. Studies have demonstrated that, even for highly resistive polyurethane and epoxy-based barrier coatings, prolonged environmental and electrochemical exposure can induce localized changes in ionic transport behavior without immediate macroscopic failure.[4-7] Such localized transport activation may significantly influence long-term durability under service conditions.

Conventional evaluation of pipeline coating performance relies on standardized durability tests such as neutral salt spray exposure, cathodic disbondment, and long-term immersion testing.[8-12] While these methods remain essential for qualification and benchmarking, they are inherently time-consuming and resource-intensive, particularly for high-build, low-permeability coating systems. Moreover, conventional tests often provide limited insight into the early-stage electrochemical degradation and transport-controlled processes that precede visible coating failure.

Electrochemical Impedance Spectroscopy (EIS) has therefore become a key non-destructive tool for assessing the protective performance of organic coatings. EIS enables quantitative evaluation of coating resistance, dielectric response, water uptake, and coating-substrate interfacial activity, providing mechanistically meaningful insight into the evolution of barrier properties during exposure.[13-17] Variations in impedance response-such as reductions in coating resistance, shifts in phase angle behavior, or the emergence of diffusion-related features-are widely interpreted as indicators of altered ionic transport and interfacial processes.

Recent investigations have further highlighted that electrochemical degradation of organic coatings is often governed by spatially localized regions of enhanced permeability, which may occupy only a small fraction of the coating area, yet dominate the overall electrochemical response under stress conditions.[18-20] Such transport inhomogeneities become particularly pronounced during accelerated electrochemical testing and under cathodic protection conditions.

To address the need for more time-efficient and mechanistically informative evaluation approaches, accelerated electrochemical protocols such as the Alternating Current-Direct Current-Alternating Current (AC-DC-AC) technique have been developed. By combining impedance measurements with controlled cathodic and/or anodic polarization steps, AC-DC-AC testing promotes alkaline attack, redox-driven interfacial reactions, and transport activation within

a significantly reduced evaluation timeframe.[21-24] Although this methodology has been successfully applied to various organic coating systems, its systematic application to thick, solvent-free, rigid polyurethane coatings used in pipeline service remains comparatively underexplored, particularly with respect to correlating accelerated electrochemical responses with long-term environmental durability.

In this study, the anticorrosive performance of a castor-oil-based, solvent-free rigid polyurethane coating formulated for pipeline steel is investigated using a combined evaluation framework involving long-term immersion EIS, AC-DC-AC accelerated electrochemical cycling, neutral salt spray exposure, and cathodic disbondment testing. By systematically comparing impedance evolution obtained under immersion, accelerated electrochemical cycling, and extended salt-spray exposure, this work aims to establish meaningful correlations between accelerated electrochemical testing and long-term corrosion performance, thereby contributing to a more application-relevant understanding of solvent-free rigid PU coatings for pipeline protection.

2. Experimental

2.1 *Materials and coatings*

A rigid solvent-free PU coating was formulated in accordance with ASTM D16, Type V, as a two-component isocyanate/polyol system. The A-component (polyol blend) consisted of castor-oil-based polyester-polyether polyols with a high hydroxyl value (220-250 mg $KOH \cdot g^{-1}$), low water content (< 0.1 wt%), and high functionality (> 2.5). This polyol composition was selected to promote the formation of a densely crosslinked polyurethane network with extensive hydrogen bonding and reduced segmental mobility, both of which are characteristics commonly associated with high barrier performance in rigid PU coatings.[25-26]

The B-component comprised a polymeric 4,4'-Diphenylmethane Diisocyanate (MDI), used as the curing agent. A stoichiometric NCO/OH ratio of 1.05 was employed to ensure near-complete conversion of reactive groups and to achieve a high network density. The mixed formulation exhibited a viscosity suitable for plural-component, airless application. Carbon steel panels (150 × 70 × 1 mm) were abrasive blast-cleaned to near-white metal condition (Sa 2 1/2) in accordance with International Organization for Standardization (ISO) 8501-1, resulting in a surface profile depth of 75 ± 5 µm. The coating components were applied using a Graco XP70 plural-component, airless spray system operated at 400 bar. Following application, the coated panels were cured for seven days under ambient laboratory conditions (23 ± 2 °C, 50 ± 5% relative humidity).

The final dry film thickness was 1,000 ± 100 µm, as measured using an Elcometer 456 digital coating-thickness gauge. Prior to electrochemical testing, all panel edges were sealed with an insulating epoxy resin to prevent electrolyte ingress from uncoated regions.

2.2 *Immersion test*

EIS was employed to evaluate the dielectric integrity, barrier performance, and degradation behavior of the solvent-free PU coating under continuous immersion conditions. Measurements were performed using a Gamry Reference 600+ potentiostat in a conventional three-electrode configuration, where the PU-coated steel panel served as the working electrode (exposed area ≈ 16 cm^2), a graphite rod was used as the counter-electrode, and an Ag/AgCl electrode (3.5 M KCl) functioned as the reference electrode.

A 5 wt% NaCl aqueous solution was selected as the electrolyte to simulate saline environments representative of buried pipelines, marine exposure, and water-contact service conditions commonly encountered in pipeline applications.[27-28] Prior to each impedance measurement, specimens were allowed to stabilize at the Open-Circuit Potential (OCP) until a steady potential was achieved, ensuring electrochemical equilibrium.

Although organic coatings are commonly characterized using small-amplitude AC perturbations (typically 10-20 mV), preliminary screening measurements indicated that the highly rigid, thick (≈ 1,000 µm), and densely crosslinked PU coating exhibited extremely low admittance. Under these conditions, conventional low-amplitude excitation resulted in an inadequate signal-to-noise ratio, particularly at low frequencies. For high-impedance organic coatings with resistances exceeding 10^9 $\Omega \cdot cm^2$, the use of elevated AC perturbation amplitudes has been reported to

significantly improve measurement stability without inducing non-linear electrochemical behavior or coating damage.[29] Accordingly, a sinusoidal perturbation amplitude of 250 mV was employed throughout this study, consistent with established recommendations for thick, highly insulating polymer coatings.[29-30]

Impedance spectra were acquired over a frequency range from 100 kHz to 0.01 Hz. Measurements were initiated after 24 h of immersion and repeated at regular intervals up to a total exposure duration of 60 days. At least three replicate specimens were tested at each immersion interval to ensure reproducibility and statistical reliability.

The non-ideal dielectric behavior commonly observed in polymeric coatings was modeled using a Constant Phase Element (CPE), accounting for distributed relaxation times arising from coating heterogeneity, surface roughness, and microstructural inhomogeneities. Coating capacitance (C_c) values were calculated from the fitted CPE parameters using the Brug equation, which is widely accepted for high-resistance organic coatings exhibiting non-ideal capacitive behavior.[31-32]

This EIS methodology enabled quantitative monitoring of coating resistance (R_{coat}), dielectric response, and the water uptake evolution over time, providing mechanistically meaningful insight into transport-controlled degradation processes in rigid, solvent-free polyurethane coatings under immersion exposure.

2.3 *AC-DC-AC test*

Accelerated degradation of the solvent-free PU coating was investigated using the AC-DC-AC electrochemical protocol, originally developed by Bierwagen, Tallman, and co-workers to simulate electrochemical stress in organic coatings subjected to cyclic polarization.[33] This methodology has been increasingly applied to polymeric coating systems, as it enables controlled acceleration of degradation mechanisms-such as electrolyte ingress, alkaline attack, and coating-substrate interfacial processes-while preserving their mechanistic relevance to long-term field exposure and significantly reducing evaluation time.[34-36]

In the present study, each AC-DC-AC cycle commenced with an EIS measurement at the OCP, followed by cathodic polarization at -10 V relative to OCP for 20 min. This cathodic potential was selected to represent severe overprotection conditions that may occur in buried steel pipelines operating under Cathodic Protection (CP), where excessive polarization can promote hydroxyl ion generation, hydrogen evolution, and increased interfacial stress at the coating-metal interface.[37-38] After completion of the cathodic polarization step, the specimens were allowed to relax at OCP, and a subsequent EIS spectrum was recorded to assess changes in coating barrier performance induced by the applied DC stress. This cycle was repeated until a pronounced decrease in low-frequency impedance or visible surface deterioration was observed.

To simulate more aggressive and fluctuating service conditions, a modified AC-DC-AC protocol was also employed. In this variant, cathodic polarization at -10 V (30 min) was followed by anodic polarization at + 10 V (30 min), with each DC step separated by an OCP relaxation period and an EIS measurement. The inclusion of anodic polarization introduces additional oxidative and metal-dissolution processes, thereby reproducing conditions such as stray-current interference, transient anodic excursions, or non-uniform CP environments encountered in pipeline systems.[39-40] Under these combined polarization conditions, both alkaline-driven degradation during cathodic steps and redox-driven interfacial reactions during anodic steps contribute to accelerated coating degradation.

Both cathodic-only and combined cathodic-anodic AC-DC-AC protocols were applied to the same coating formulation, enabling direct comparison of degradation pathways. The evolution of impedance parameters-including coating resistance, capacitance, and the emergence of additional time constants-was analyzed to elucidate the mechanisms governing barrier deterioration, water and ion transport, and coating-metal interfacial reactions. This comparative approach provides a robust framework for assessing the electrochemical durability of rigid, solvent-free PU coatings and for evaluating the predictive capability of AC-DC-AC testing with respect to long-term corrosion performance in pipeline applications.

2.4 *Cathodic disbonding test*

The compatibility of the solvent-free PU coating with CP conditions was evaluated using the Cathodic Disbondment (CD) test in accordance with American Water Works Association (AWWA) C222. CD testing provides insight into the resistance of a coating to alkaline environments and hydrogen evolution that occur when steel pipelines

are protected electrochemically.

A circular holiday (defect) with a diameter of 6 mm was introduced into the coating to expose the underlying steel substrate. The coated panels were immersed in a 3 wt% NaCl solution and polarized at -1.4 V vs. Ag/AgCl for 28 days at 23 ± 2 °C.

After exposure, the disbonded coating surrounding the defect was carefully removed using a plastic scraper, and the radial disbondment distance was measured along four orthogonal directions. According to the acceptance criteria defined in AWWA C222, a maximum mean radial disbondment radius of ≤ 10 mm is required for coatings intended for buried pipeline applications.

This test provides a direct assessment of coating resistance to CP-induced alkaline degradation and complements the electrochemical findings obtained from EIS and AC-DC-AC testing, allowing correlation between interfacial stability under cathodic polarization and long-term adhesion performance.

2.5 *Neutral salt spray test*

The long-term corrosion resistance of the solvent-free polyurethane coating was evaluated using the Neutral Salt Spray (NSS) test in accordance with ISO 9227. Coated steel panels were placed in a CW Specialist SF-1000A salt spray chamber (internal volume: 1,000 L) and positioned at an inclination angle of 20° from the vertical, as specified by the standard, to ensure uniform salt deposition on the coating surface. A continuous fog of 5 wt% NaCl solution was applied at 35 °C, while the relative humidity inside the chamber was maintained between 95 and 100%. The total exposure duration was 2,500 h, corresponding to an extended accelerated corrosion test commonly employed for qualification and comparative evaluation of pipeline coating systems. Panels were periodically removed after 240, 480, 720, 1,000, and 1,200 h, and at the final exposure time of 2,500 h for visual assessment of coating degradation. Blistering, rusting, cracking, and flaking were evaluated in accordance with ISO 4628 (Parts 2-5).

In addition to visual inspection, EIS measurements were performed on selected panels following NSS exposure. This combined evaluation enabled correlation between macroscopic coating defects and changes in electrochemical barrier properties, providing complementary insight into the evolution of coating degradation during long-term salt spray exposure and allowing direct comparison with trends observed in accelerated AC-DC-AC testing.

3. Results and discussion

3.1 *Immersion test*

Figure 1 presents the Bode magnitude (|Z|) and phase angle-plots of the 1,000-µm-thick rigid solvent-free PU coating during immersion in 5 wt% NaCl for up to 60 days. Throughout the entire exposure period, the phase angle remains close to -90° over a broad frequency range, indicating a predominantly capacitive response governed by the coating layer. No secondary phase maximum or additional low-frequency relaxation process is observed, suggesting that electrolyte ingress remains confined within the bulk coating and that no significant interfacial charge-transfer activity develops within the investigated exposure period.

This single-time-constant behavior is characteristic of dense polymeric barrier coatings with restricted ionic transport and limited segmental mobility, and has been widely reported for intact polyurethane and epoxy systems under immersion conditions.[41-43] The absence of additional low-frequency features throughout immersion further confirms that the coating retains its dielectric integrity and effectively suppresses corrosion activity at the steel substrate.

Accordingly, all impedance spectra were fitted using a single-time-constant equivalent circuit model consisting of a R_{coat} in parallel with a CPE, as shown in Figure 2. Initial fitting attempts using an ideal capacitor resulted in systematic deviations between experimental and simulated spectra, indicating non-ideal dielectric behavior of the coating. Therefore, the capacitor was replaced by a CPE to account for distributed relaxation times arising from coating heterogeneity, thickness variations, and microstructural inhomogeneities. The fitted CPE parameters (Q and n) were obtained directly from the software, with the CPE exponent ($n < 1$) reflecting the deviation from ideal capacitive behavior. For comparative analysis, equivalent C_c values were derived from the fitted CPE parameters using the Brug relationship, as commonly applied for high-resistance organic coatings.[44,45]

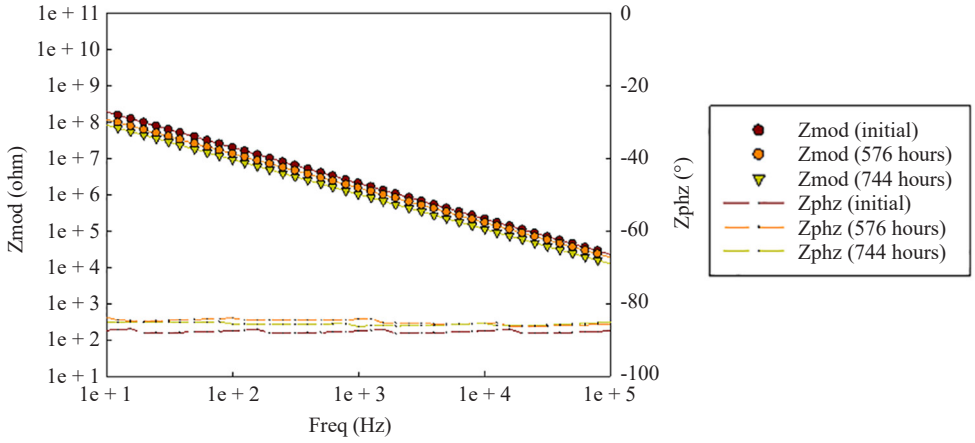

Figure 1. Typical EIS Bode spectra (impedance modulus and phase angle) for the solvent-free polyurethane/steel system in the test solution

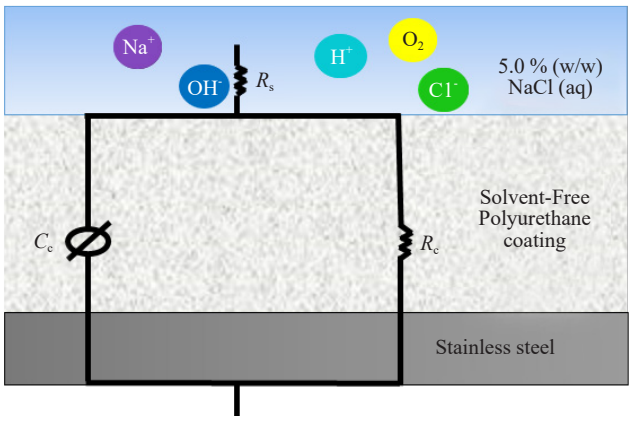

Figure 2. The corresponding equivalent circuit model used for data fitting

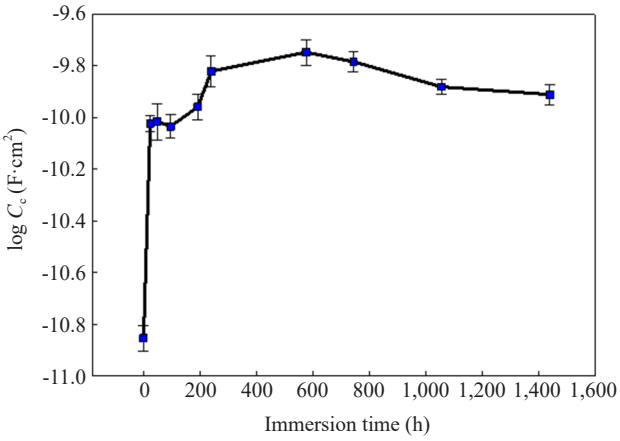

Figure 3. The evolution of C_c with time for the solvent-free polyurethane coating at different immersion times

The evolution of the logarithmic C_c (log C_c) with immersion time is shown in Figure 3. The log C_c values exhibit only a slight increase over the exposure period, indicating limited water uptake and minimal dielectric degradation of

the coating. The absolute capacitance values remain on the order of 10^{-9} F·cm^{-2}, consistent with a compact dielectric structure and restricted electrolyte transport within the polymer matrix.

The low-frequency impedance modulus ($|Z|_{0.01}$ Hz) remained above 10^8 Ω·cm^2 even after 744 h of immersion (Figure 4), confirming excellent barrier performance. The R_{coat} values obtained from fitting exhibited only minor variations over time, further reflecting the dense polymer network and low permeability of the rigid PU coating.

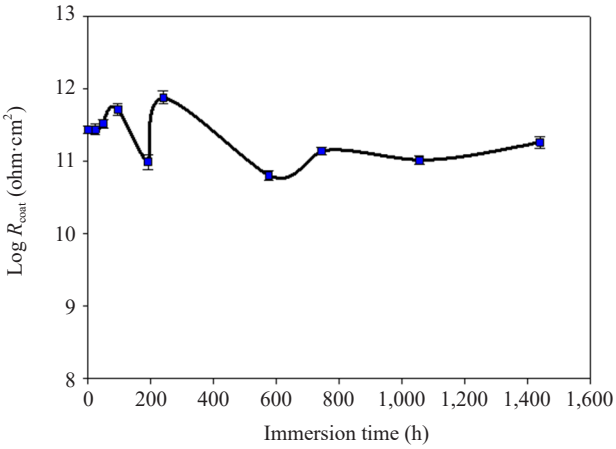

Figure 4. The evolution of low-frequency impedance modulus ($|Z|_{0.01}$ Hz) with time for the solvent-free polyurethane coating at different immersion times

Water absorption, calculated using the Brasher-Kingsbury relationship,[46] reached a maximum value of approximately 2.1% after 60 days of immersion. This relatively low uptake is consistent with solvent-free rigid polyurethane systems, where the hydrophobic chain structure and high crosslink density reduce free volume and restrict diffusive transport. In organic coating systems, significant degradation and interfacial corrosion are typically reported when coating resistance decreases below approximately 10^5 Ω·cm^2 or when coating capacitance exceeds ~ 10^{-6} F·cm^{-2}, indicating extensive electrolyte penetration and loss of barrier function.[41-43] In the present study, neither threshold was approached at any immersion time point, further supporting that the coating remains electrochemically intact under prolonged immersion conditions.

All impedance parameters were obtained from area-normalized fitting performed by the software using the exposed electrode area entered for each specimen. The quality of the fitting was verified through residual analysis and coefficients of determination ($R^2 > 0.98$) for all datasets, confirming the robustness and physical relevance of the selected model for describing the EIS response of thick, highly insulating polyurethane coatings.

3.2 *AC-DC-AC test*

The accelerated degradation behavior of the solvent-free rigid PU coating was investigated using the cathodic-only AC-DC-AC protocol, consisting of cyclic cathodic polarization (-10 V vs. OCP) followed by relaxation at open-circuit potential and subsequent impedance measurements. This protocol was designed to simulate severe cathodic overprotection conditions that may occur in buried steel pipelines operating under cathodic protection systems.

During the initial stage of AC-DC-AC cycling, the impedance response remained coating-dominated, closely resembling the behavior observed during simple immersion exposure. Up to approximately 100 h of cycling, the Bode phase angle remained near -90° over a wide frequency range, indicating a predominantly capacitive response controlled by the coating layer (Figure 5). In this regime, electrolyte ingress was largely confined within the bulk coating, and no clear indication of interfacial electrochemical activity was observed.

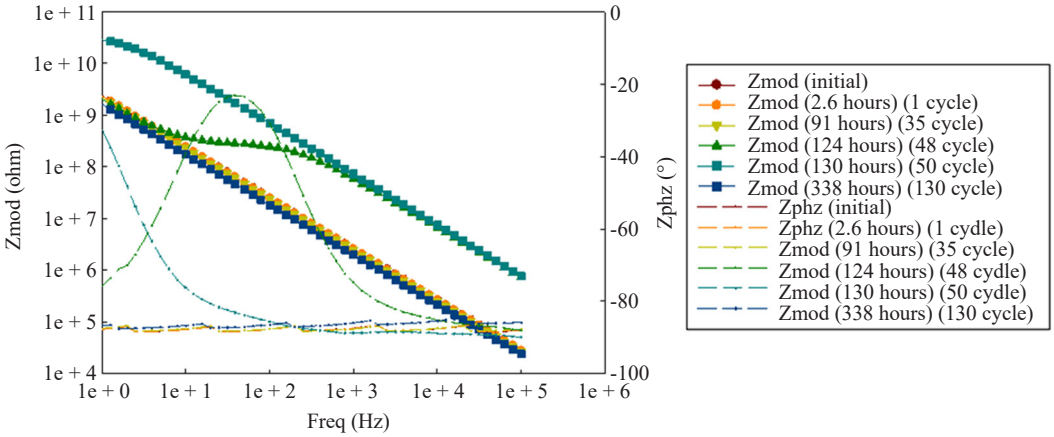

Figure 5. Typical EIS Bode spectra for the solvent-free polyurethane/steel system during cathodic-only AC-DC-AC cycling

With continued cathodic polarization, a pronounced degradation stage developed. Between approximately 100 and 170 h of cycling, the R_{coat} decreased significantly, reaching values on the order of 10^4-10^5 Ω·cm^2 (Figure 6). This behavior reflects enhanced ionic transport and electrolyte accumulation within the coating under sustained alkaline conditions generated by cathodic polarization. During this stage, the impedance response transitioned toward a diffusion-influenced regime, indicating partial wetting of the coating-steel interfacial region rather than the onset of fully charge-transfer-controlled corrosion processes (Figure 7).

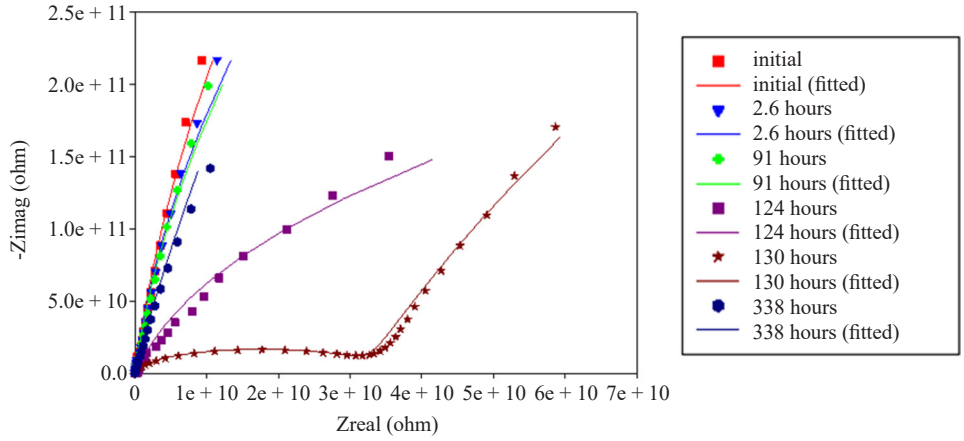

Figure 6. EIS Nyquist spectra for the solvent-free polyurethane coating at different AC-DC-AC cycling times

Importantly, no recovery of barrier properties was observed within the 120-170 h interval. The coating remained in a degraded state characterized by low R_{coat} values and diffusion-influenced impedance behavior. This observation confirms that the apparent stabilization reported in earlier interpretations does not occur during this intermediate exposure period.

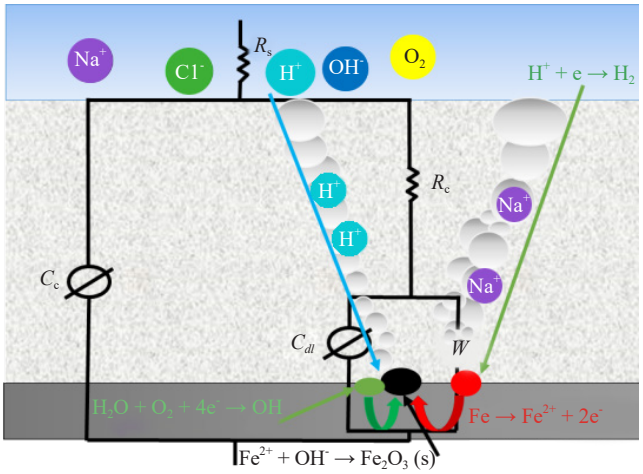

Figure 7. The corresponding equivalent circuit model used for data fitting

At extended cycling times, a distinct pseudo-recovery behavior emerged. At approximately 300 h of AC-DC-AC exposure, the coating resistance increased to the 10^6-10^7 $\Omega \cdot cm^2$ range, and the impedance response became more coating-dominated (Table 1). This delayed increase in R_{coat} does not indicate true restoration or healing of the polymer barrier. Instead, it is attributed to the accumulation of corrosion products and interfacial deposits, such as iron hydroxides and oxides, formed under prolonged cathodic polarization. These products can partially block ionic transport pathways and reduce effective diffusivity within the wetted interfacial region, leading to a transient increase in impedance.

Table 1. Evolution of model parameters (R_c and C_c) for the solvent-free polyurethane coating as a function of AC-DC-AC cycling time

Time (h)	R_s ($\Omega \cdot cm^2$)	C_c ($\Omega^{-1} \cdot cm^{-2} \cdot s$)	R_{coat} ($\Omega \cdot cm^2$)	C_{edL} ($\Omega^{-1} \cdot cm^{-2} \cdot s$)	W
İnitial	454.6	6.8E-11	5.8E + 12		
2.6	433.8	6.8E-11	6.0E + 12		
13	439.1	7.0E-11	6.6E + 12		
119.6	389.4	2.7E-12	9.4E + 08	7.4E-11	1.2E-14
169	0.7	5.2E-11	5.0E + 04	4.5E-11	1.2E-15
299	578.9	9.7E-11	6.5E + 6	4.9E-12	1.3E-12
351	820.2	9.6E-12	4.2E + 6	7.5E-12	1.1E-12

The impedance spectra recorded at 338 h are consistent with this pseudo-recovery stage. Although the Bode response at this time appears similar to early-stage behavior, it represents a fundamentally different physical state governed by diffusion blockage rather than intact barrier properties. As such, the apparent similarity between the 338 h spectra and the initial response should not be interpreted as genuine barrier recovery but rather as a consequence of interfacial transport limitation.

Overall, the cathodic-only AC-DC-AC response of the solvent-free PU coating can be divided into three distinct stages:

(i) an initial coating-controlled stage with predominantly capacitive behavior (≤ 100 h);

(ii) a degradation stage characterized by significant R_{coat} reduction and diffusion-influenced transport (≈ 100-170 h);

and,

(iii) a delayed pseudo-recovery stage at extended exposure times (≈ 300 h), associated with corrosion product accumulation and partial blockage of ionic pathways.

These results demonstrate that prolonged cathodic polarization induces substantial degradation of the solvent-free PU coating while delaying the transition to fully active interfacial corrosion. The observed non-monotonic impedance evolution highlights the importance of time-resolved interpretation of AC-DC-AC data and provides mechanistically meaningful insight into coating behavior under cathodic overprotection conditions relevant to pipeline applications.

3.3 *Modified AC-DC-AC test*

The modified AC-DC-AC protocol, incorporating alternating cathodic (-10 V) and anodic (+ 10 V) polarization steps, produced a distinctly different degradation response compared to the cathodic-only cycling regime. Unlike the standard AC-DC-AC protocol, which predominantly promotes alkaline stress and hydrogen evolution, the combined polarization sequence imposes cyclic redox conditions that simultaneously activate alkaline-induced polymer swelling during cathodic steps and anodic-induced metal dissolution processes at the coating-steel interface.

As shown in Figure 8, the impedance response initially exhibited a single dominant time constant, closely resembling the early-stage behavior observed during both immersion testing and cathodic-only AC-DC-AC cycling. However, after approximately 30-40 h of cycling, the Bode phase spectra evolved into a two-time-constant system, indicating the onset of interfacial electrochemical activity in addition to bulk coating degradation. In this regime, the high-frequency response remained associated with the dielectric properties of the polyurethane coating, whereas the emerging mid- to low-frequency responses reflects electrochemical processes occurring at the coating-metal interface.

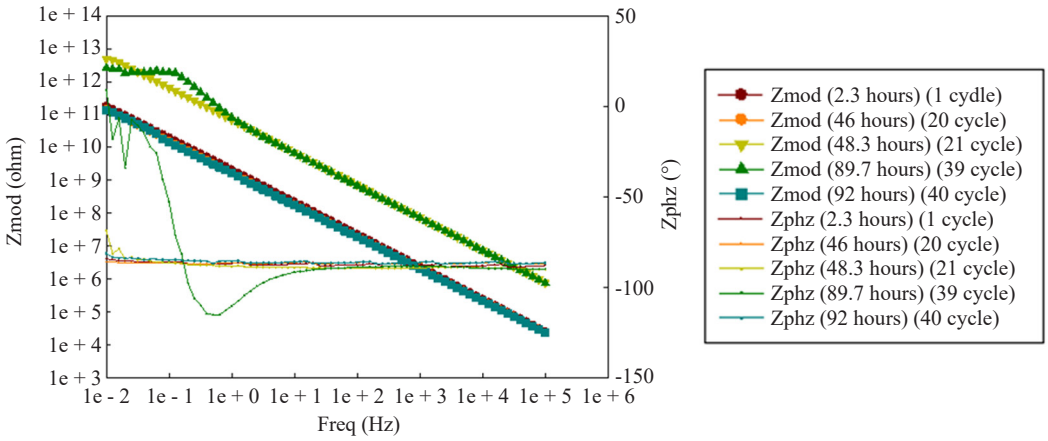

Figure 8. Typical EIS Bode spectra and phase diagram for the solvent-free polyurethane/steel system during combined cathodic-anodic AC-DC-AC cycling

The corresponding Nyquist plots (Figure 9) provide further mechanistic insight into this transition. The initially large, coating-dominated semicircle progressively contracted with continued cycling, while a second, depressed arc accompanied by a low-frequency diffusion tail became increasingly evident. The slope of the low-frequency region approached the characteristic 45° behavior, indicating the development of diffusion-controlled transport. This behavior was successfully captured in the equivalent circuit model by the inclusion of a Warburg diffusion element. Notably, such a diffusion component was absent in the immersion EIS results and was not required during the early stages of the cathodic-only AC-DC-AC test, confirming that its emergence is directly associated with the combined cathodic-anodic polarization sequence.

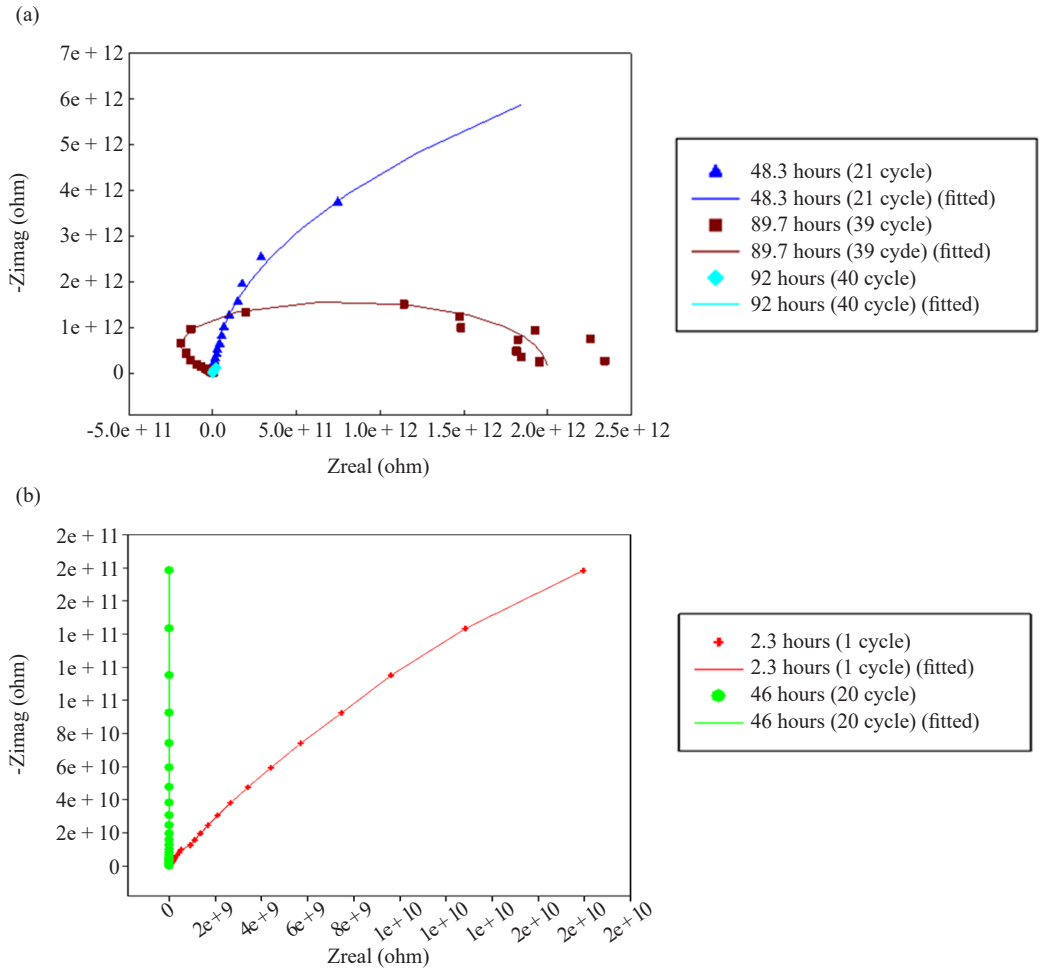

Figure 9. EIS Nyquist spectra for the solvent-free polyurethane coating at different AC-DC-AC cycling times

Quantitative analysis revealed that the fitted R_{coat} decreased by approximately six orders of magnitude, from initial values on the order of 10^{11}-10^{12} Ω·cm^2 to approximately 10^5-10^6 Ω·cm^2 after 40-50 cycles (Table 2). Despite this pronounced reduction, a stabilization plateau was observed at extended cycling times, with R_{coat} remaining within the 10^6 Ω·cm^2 range. This apparent stabilization is consistent with the accumulation of corrosion products, such as FeOOH, Fe_2O_3, and Fe_3O_4, within confined interfacial regions. These products can temporarily hinder further ionic diffusion and partially block transport pathways under alternating redox conditions, leading to transient impedance stabilization rather than permanent barrier recovery.

Optical microscopy images (Figure 10) corroborate the electrochemical observations, revealing localized blistering, microcracking, and pigment displacement in regions subjected to combined polarization. The observed defect morphology supports a synergistic degradation mechanism involving alkaline-driven blister formation during cathodic steps and metal-dissolution-reprecipitation processes during anodic polarization. This interplay explains both the earlier onset of interfacial activity and the pronounced diffusion-controlled impedance features relative to the cathodic-only AC-DC-AC regime.

Overall, the modified AC-DC-AC protocol induced significantly accelerated degradation kinetics and more complex impedance signatures than the cathodic-only cycling. The clear emergence of a second time constant and a Warburg diffusion element highlights the sensitivity of this approach for probing interfacial transport and corrosion processes in high-build, solvent-free polyurethane coatings. These results demonstrate that combined cathodic-anodic polarization cycling provides a more realistic and mechanistically informative simulation of field conditions, in which coated pipelines may experience fluctuating cathodic protection levels, stray currents, and transient anodic excursions.

Table 2. Evolution of R_{coat} for the solvent-free polyurethane coating as a function of AC-DC-AC cycling time

Time (h)	R_s ($\Omega \cdot cm^2$)	C_c ($\Omega^{-1} \cdot cm^{-2} \cdot s$)	R_{coat} ($\Omega \cdot cm^2$)	C_{edL} ($\Omega^{-1} \cdot cm^{-2} \cdot s$)	n	W
İnitial	1.96	7.6E-11	1.9E + 12			
2.3	2.1E + 00	8.0E-11	1.9E + 12			
4.6	2.3E-02	8.0E-11	3.0E-11			
39.1	1.3	1.0E-11	5.6E + 12			
41.4	2.5E-03	2.8E-12	3.4E + 10	7.4E-11	9.2E-1	1.2E-14
87.4	313.1	1.1E-10	21.9E + 6	2.3E-12	9.5E-3	1.1E-13
119.6	5.1E-2	8.6E-11	10.6E + 3	2.5E-11	9.9E-3	5.5E-14
170.2	7.2E-4	7.9E-11	8.2E + 3	3.2E-11	9.7E-3	8.5E-15

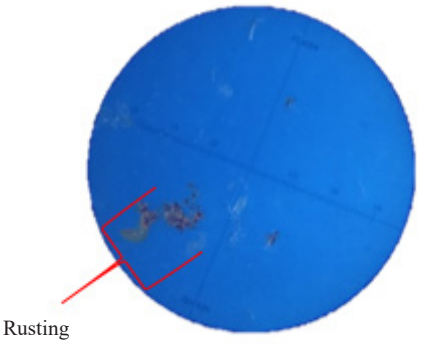

Figure 10. Optical microscopy image of the polyurethane coating after 40 cycles of AC-DC-AC testing, showing localized blistering and microcracking

3.4 *Cathodic disbondment*

CD testing was performed to evaluate the compatibility of the solvent-free rigid PU coating with CP conditions commonly applied to buried steel pipelines. Under CP, cathodic polarization induces the generation of hydroxyl ions (OH^-) and hydrogen evolution at the steel surface, which may weaken coating adhesion or promote blistering if ionic transport through the coating is significant. Therefore, CD testing provides a critical assessment of a coating's resistance to alkaline attack and interfacial degradation under electrochemical stress.

The test was conducted in accordance with AWWA C222, using coated steel panels with a nominal dry film thickness of approximately 960-990 µm. A controlled circular holiday was introduced at the coating center to expose the steel substrate. The panels were immersed in a 3 wt% NaCl electrolyte and polarized at -1.50 V vs. Ag/AgCl for 28 days at 23 ± 2 °C, consistent with severe cathodic overprotection conditions.

After exposure, the disbonded coating surrounding the holiday was carefully removed, and the disbondment diameter was measured along multiple radial directions for each panel. The measured disbondment diameters ranged between approximately 12.0 and 15.3 mm, corresponding to mean radial disbondment values of ~5.0-6.0 mm (Table 3). According to AWWA C222 acceptance criteria, coatings intended for buried pipelines must exhibit a maximum mean radial disbondment of ≤ 10 mm. All tested panels therefore fully satisfied the standard requirements, despite the aggressive polarization potential applied.

Table 3. Cathodic disbondment results of the solvent-free rigid polyurethane coating after 28 days of exposure (at -1.50 V vs. Ag/AgCl)

Panel number	1	2	3
DFT mean	960 ± 25	980 ± 20	990 ± 15
Exposure *E* (V)	-1.50	-1.50	-1.50
Disbondment diameter (mm)	12.2	12.4	14.0
	12.0	12.3	14.3
	12.4	12.5	14.3
	12.2	12.2	15.3
Mean radius (mm)	5.5 ± 0.4	5.3 ± 0.6	5.6 ± 0.2

Panel-to-panel variations were observed, with slightly higher disbondment values recorded for Panel 3. This variation is attributed to local differences in coating thickness, holiday geometry, and interfacial stress concentration rather than a systematic loss of coating performance. Importantly, even in the most severe case, the radial disbondment remained well below the acceptance threshold, indicating that interfacial adhesion was largely preserved.

The limited extent of cathodic disbondment is consistent with the coating's dense, highly crosslinked polymer network, which restricts OH^- transport and suppresses extensive underfilm alkalization. This behavior correlates well with the immersion EIS results, which showed sustained high coating resistance and low capacitance, and with the AC-DC-AC tests, where degradation progressed gradually and stabilization phenomena were observed rather than a catastrophic interfacial failure.

Overall, the CD results confirm that the solvent-free rigid PU coating maintains strong adhesion and electrochemical stability under severe cathodic protection conditions. The combination of low radial disbondment, high-build film integrity, and consistent electrochemical performance demonstrates the coating's suitability for long-term protection of buried steel pipelines subjected to cathodic protection.

3.5 *NSS test*

The long-term corrosion resistance of the solvent-free rigid PU coating was further evaluated under NSS exposure in accordance with ISO 9227 for a total duration of 2,500 h. During the test period, coated panels were periodically inspected for blistering, rust formation, cracking, flaking, and under-film corrosion propagation from the intentionally introduced scribe.

Throughout the entire exposure duration, intact coating areas exhibited excellent visual stability. Blistering and rust ratings evaluated according to ISO 4628-2 and ISO 4628-3 remained at the highest classification levels (0(S0) and Ri0, respectively), while no cracking or flaking was detected in accordance with ISO 4628-4 and ISO 4628-5. These observations indicate the absence of significant osmotic blistering, coating embrittlement, or cohesive failure within the polyurethane matrix, even under prolonged chloride-rich exposure (Table 4).

Table 4. Visual evaluation of the solvent-free rigid polyurethane coating according to ISO 4628 after NSS exposure

Exposure time (h)	Blistering according to TS EN ISO 4628-2	Rust grade according to TS EN ISO 4628-3	Cracking according to TS EN ISO 4628-4	Flaking according to TS EN ISO 4628-5
240	0(S0)	Ri0	0(S0)	0(S0)
480	0(S0)	Ri0	0(S0)	0(S0)
720	0(S0)	Ri0	0(S0)	0(S0)
1,000	0(S0)	Ri0	0(S0)	0(S0)
2,500	0(S0)	Ri0	0(S0)	0(S0)

After extended NSS exposure, slight rust staining was observed in the immediate vicinity of the (Figure 11). However, corrosion propagation remained confined close to the defect edges and did not advance significantly into the surrounding coated regions. This behavior is consistent with the hydrophobic nature of the polyurethane network, which primarily limits water affinity and lateral electrolyte transport, while the rigid and highly cross-linked structure contributes secondarily by restricting segmental mobility. As a result, under-film corrosion was effectively suppressed even under continuous salt fog conditions.

Figure 11. Macroscopic image of the solvent-free rigid polyurethane coating after 2,500 h of neutral salt spray (NSS) exposure

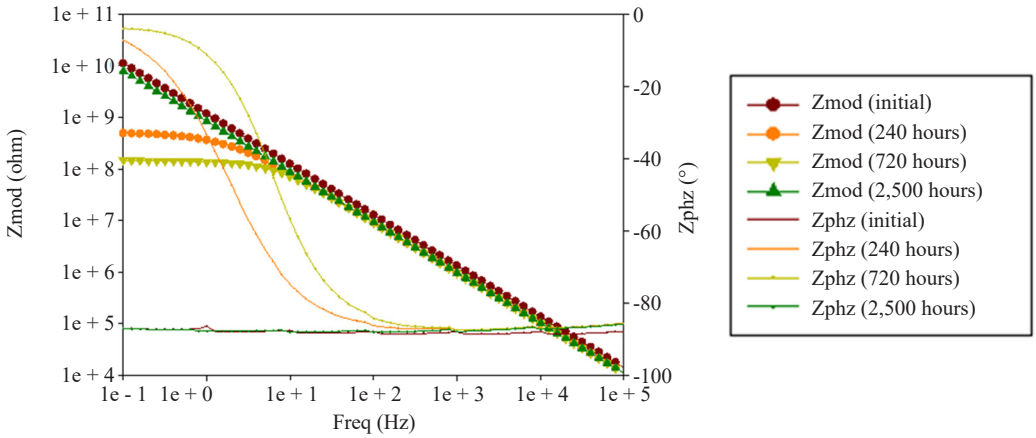

Figure 12. Typical EIS Bode spectra for the solvent-free polyurethane/steel system at different NSS test times

Electrochemical impedance spectroscopy performed on specimens periodically removed from the NSS chamber corroborated the visual observations. The impedance modulus at 0.01 Hz remained above 10^6 Ω·cm^2 after 2,500 h of exposure, indicating that the coating continued to provide effective barrier protection. Although the R_{coat} decreased progressively from its initial high values (>10^{11} Ω·cm^2), it stabilized within the 10^6-10^7 Ω·cm^2 range at extended exposure times, reflecting a transition toward diffusion-limited transport rather than the development of fully active interfacial corrosion processes (Figure 12 and Figure 13).

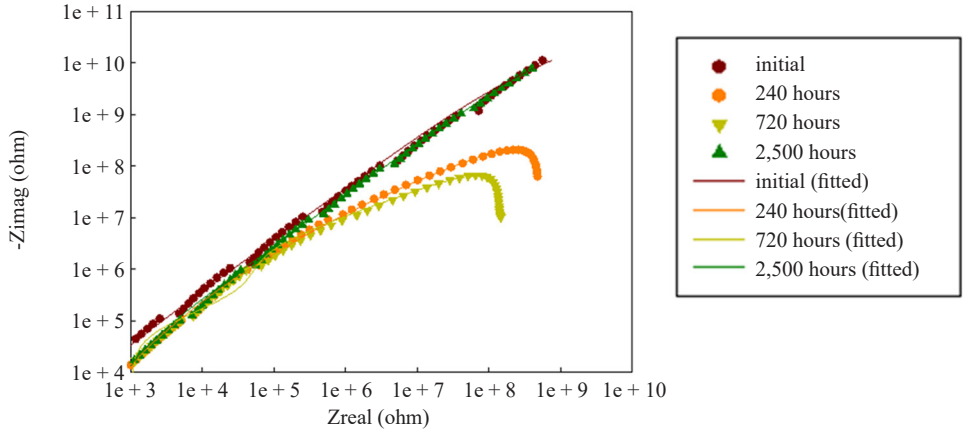

Figure 13. EIS Nyquist spectra for the solvent-free polyurethane coating at different NSS test times

Notably, this apparent stabilization behavior closely mirrors the impedance evolution observed during AC-DC-AC accelerated electrochemical cycling. In both cases, an initial rapid decline in R_{coat} was followed by a plateau region, which is attributed to the accumulation of corrosion products at the coating-steel interface. These products partially block ionic transport pathways, thereby limiting further degradation without indicating true restoration of the coating barrier.

The strong correspondence between the impedance stabilization observed after approximately 60-70 AC-DC-AC cycles and that measured after 2,500 h of NSS exposure provides compelling evidence that the accelerated electrochemical protocol captures the dominant degradation mechanisms governing long-term coating performance. This correlation is particularly valuable for high-build, solvent-free PU coatings, for which conventional salt spray testing requires extended durations and substantial experimental resources (Table 5).

Overall, the NSS results confirm that the solvent-free rigid PU coating maintains effective barrier integrity and corrosion resistance under aggressive chloride exposure. When interpreted together with immersion EIS and AC-DC-AC data, these findings demonstrate that accelerated electrochemical testing serves as a reliable and mechanistically meaningful tool for predicting the long-term service performance of solvent-free polyurethane coatings in pipeline applications.

Table 5. The evolution of model parameters (R_{coat} and C_c) for the solvent-free polyurethane coating during the NSS test

Time (h)	R_s ($\Omega \cdot cm^2$)	C_c ($\Omega^{-1} \cdot cm^{-2} \cdot s$)	R_{coat} ($\Omega \cdot cm^2$)	C_{edl} ($\Omega^{-1} \cdot cm^{-2} \cdot s$)	W
Initial	124.1	1.4E-10	2.8E + 11		
240	480	2.1E-10	3.3E + 08	2.8E-09	1.93E-09
410	476.7	2.1E-10	1.4E + 08	1.9E-08	8.14E-08
850	415.5	1.8E-10	1.6E + 06	1.0E-11	4.90E-12
2,500	5.48E-04	1.E-10	6.2E + 06	4.7E-11	7.40E-11

4. Conclusion

This study systematically evaluated the anticorrosive performance of a rigid solvent-free PU coating using an integrated assessment framework combining long-term immersion EIS, AC-DC-AC accelerated electrochemical

cycling, and conventional durability tests, including cathodic disbondment and NSS exposure. During immersion in 5 wt% NaCl, the coating exhibited consistently high barrier resistance, with R_{coat} values remaining above 10^8 Ω·cm^2 and low water uptake. This behavior reflects the predominantly hydrophobic nature of the polyurethane network, which limits water affinity and continuous ionic pathways, while network rigidity and crosslink density contribute secondarily by restricting segmental mobility and transport rates. The persistence of a single time constant throughout immersion confirmed that electrolyte ingress remained confined within the coating bulk and did not activate interfacial corrosion processes.

Under accelerated electrochemical stress, distinct impedance evolution patterns were observed depending on the applied polarization protocol. Cathodic-only AC-DC-AC cycling primarily promoted alkaline-driven degradation and diffusion-limited transport processes, whereas combined cathodic-anodic cycling induced a faster onset of interfacial electrochemical activity and more complex impedance responses. Despite these differences, both protocols exhibited an apparent, diffusion-limited stabilization of impedance parameters at extended cycling times. This behavior is attributed to the accumulation of corrosion products at the coating-steel interface, which partially restrict ionic transport pathways rather than indicating true recovery or restoration of the coating barrier.

Cathodic disbondment testing confirmed the coating's compatibility with cathodic protection systems, with disbondment values remaining well within the acceptance limits specified by AWWA C222. Prolonged NSS exposure (2,500 h) resulted in minimal blistering and rusting, and impedance measurements performed after NSS testing exhibited trends closely aligned with those obtained during AC-DC-AC cycling. This strong correspondence demonstrates that the accelerated electrochemical protocol captures key degradation mechanisms governing long-term environmental performance of the coating.

Overall, the findings demonstrate that solvent-free rigid PU coatings provide durable and effective corrosion protection for pipeline applications, benefiting from their VOC-free formulation, hydrophobic polymer architecture, and resistance to transport-controlled degradation. Importantly, this work establishes AC-DC-AC electrochemical cycling as a mechanistically meaningful and resource-efficient complementary tool for predicting long-term coating performance, thereby contributing to the development, qualification, and sustainability assessment of protective coating systems for infrastructure applications.

Conflict of interest

The authors declare no competing financial interest.

References

[1] Bierwagen, G. P.; Tallman, D. E.; Li, J.; He, L.; Jeffcoate, C. S. EIS studies of coated metals in accelerated exposure. *Prog. Org. Coat.* **2003,** *46*, 149-158.

[2] Bierwagen, G.; Tallman, D.; Li, J.; He, L.; Jeffcoate, C. EIS studies of coated metals in accelerated exposure. *Prog. Org. Coat.* **2003,** *46*(2): 149-158.

[3] Lyon, S. B.; Bingham, R.; Mills, D. J. Advances in corrosion protection by organic coatings. *Prog. Org. Coat.* **2017,** *102*, 2-7.

[4] Usman, B. J.; Scenini, F.; Curioni, M. Exploring the use of an AC-DC-AC technique for the accelerated evaluation of anticorrosion performance of anodic films on aluminium alloys. *Prog. Org. Coat.* **2020,** *144*, 105648.

[5] Brasher, D. M.; Kingsbury, A. H. Electrical measurements in the study of immersion degradation of coatings. *J. Appl. Chem.* **1954,** *4*, 62-72.

[6] International Organization for Standardization. *Corrosion Tests in Artificial Atmospheres-Salt Spray Tests*; ISO 9227:2022; ISO: Geneva, 2022.

[7] International Organization for Standardization. *Paints and Varnishes-Evaluation of Degradation of Coatings*; ISO 4628 (Parts 1-5); ISO: Geneva, 2016.

[8] ASTM International. *Standard Test Methods for Cathodic Disbondment of Pipeline Coatings*; ASTM G8-96(2019); ASTM International: West Conshohocken, PA, 2019.

[9] ASTM International. *Standard Test Method for Evaluation of Painted or Coated Specimens*; ASTM D1654-

08(2016); ASTM International: West Conshohocken, PA, 2016.
[10] ASTM International. *Standard Test Method for Pull-Off Strength of Coatings*; ASTM D4541-17; ASTM International: West Conshohocken, PA, 2017.
[11] Amirudin, A.; Thierry, D. Application of electrochemical impedance spectroscopy to study the degradation of polymer-coated metals. *Prog. Org. Coat.* **1995,** *26*, 1-28.
[12] Bierwagen, G. P.; Allahar, K. N.; Su, Q.; Gelling, V. J. Electrochemically characterizing the AC-DC-AC accelerated test method using embedded electrodes. *Corros. Sci.* **2009,** *51*, 95-101.
[13] Allahar, K. N.; Upadhyay, V.; Bierwagen, G. P. Characterizing the relaxation of the open-circuit potential during an AC-DC-AC accelerated test. *Corrosion* **2010,** *66*(9), 095001.
[14] Xu, M.; Lam, C. N. C.; Wong, D.; Asselin, E. Evaluation of the cathodic disbondment resistance of pipeline coatings-A review. *Prog. Org. Coat.* **2020,** *146*, 105728.
[15] Mahdavi, F.; Tan, M. Y. J.; Forsyth, M. Electrochemical impedance spectroscopy as a tool to measure cathodic disbondment on coated steel surfaces: Capabilities and limitations. *Prog. Org. Coat.* **2015,** *88*, 23-31.
[16] Margarit, I. C. P.; Mattos, O. R.; Ferreira, J. R. R. M.; Quintela, J. P. About coatings and cathodic protection: Electrochemical features of coatings used on pipelines. *J. Coat. Technol.* **2001,** *73*, 61-65.
[17] Brasher, D. M.; Kingsbury, A. H. Electrical measurements in the study of immersed paint coatings on metal. I. Comparison between capacitance and gravimetric methods of estimating water uptake. *J. Appl. Chem.* **1954,** *4*, 62-72.
[18] Wen, C.; Li, J.; Wang, S.; Yang, Y. Experimental study on stray current corrosion of coated pipeline steel. *J. Nat. Gas Sci. Eng.* **2015,** *27*, 1555-1561.
[19] Wen, J. G.; Geng, W.; Geng, H. Z.; Zhao, H.; Jing, L. C.; Yuan, X. T.; Tian, Y.; Wang, T.; Ning, Y. J.; Wu, L. Improvement of corrosion resistance of waterborne polyurethane coatings by covalent and noncovalent grafted graphene oxide nanosheets. *ACS Omega* **2019,** *4*(23), 20265-20274.
[20] Trentin, A.; Pakseresht, A.; Duran, A.; Castro, Y.; Galusek, D. Electrochemical characterization of polymeric coatings for corrosion protection: A review. *Polymers* **2022,** *14*, 2306.
[21] Song, G. L. Modification, degradation and evaluation of a few organic coatings used for marine applications. *Corros. Mater. Degrad.* **2020,** *1*(3), 19.
[22] Liang, H.; Wu, Y.; Han, B.; Lin, N.; Wang, J.; Zhang, Z.; Guo, Y. Corrosion of buried pipelines by stray current in electrified transportation systems: Mechanisms and protection. *Applied Sciences* **2024,** *15*(1), 264.
[23] Condini, A.; Trentalange, C.; Giuliani, A.; Cristoforetti, A.; Rossi, S. Advancing corrosion protection in confined spaces: A solvent-free UV LED-curable coating for steel pipelines with enhanced barrier properties and harsh environment performance. *J. Coat. Technol. Res.* **2024,** *21*, 2009-2022.
[24] Usman, B. J.; Scenini, F.; Curioni, M. Exploring the use of an AC-DC-AC technique for the accelerated evaluation of anticorrosion performance of anodic films on aluminium alloys. *Prog. Org. Coat.* **2020,** *144*, 105648.
[25] Yang, H. Q.; Zhang, Q.; Li, Y. M.; Liu, G.; Huang, Y. Effects of mechanical stress and cathodic protection on the performance of a marine organic coating on mild steel. *Surf. Coat. Technol.* **2021,** *261*, 124233.
[26] Cui, Y.; Shen, T.; Ding, Q. Study on the influence of AC stray current on X80 steel with coating defects in simulated soil solution. *Int. J. Corros.* **2019,** *2019*, 4372430.
[27] Guo, Y. B.; Liu, C.; Wang, D. G.; Liu, S. H. Effects of alternating current interference on corrosion of X60 pipeline steel. *Pet. Sci.* **2015,** *12*, 316-324.
[28] Qian, S.; Cheng, Y. F. Degradation of fusion bonded epoxy pipeline coatings in the presence of direct current interference. *Prog. Org. Coat.* **2018,** *120*, 79-87.
[29] Parks, J.; Leidheiser, H. Ionic migration through organic coatings and its consequences to corrosion. *Ind. Eng. Chem. Prod. Res. Dev.* **1986,** *25*, 1-6.
[30] Rodriguez, R. E.; Trautman, B. L.; Payer, J. H. Influencing factors in cathodic disbondment of fusion bonded epoxy coatings. In *CORROSION 2000*. Association for Materials Protection and Performance: Orlando, FL, 2000; pp 1-14.
[31] Stafford, O. A.; Hinderliter, B. R.; Croll, S. G. Electrochemical impedance spectroscopy response of water uptake in organic coatings by finite element methods. *Electrochim. Acta* **2006,** *52*(3): 1339-1348.
[32] Bonora, P. L.; Deflorian, F.; Fedrizzi, L. Electrochemical impedance spectroscopy as a tool for investigating underpaint corrosion. *Electrochim. Acta* **1996,** *41*, 1073-1082
[33] Mansfeld, F. Use of electrochemical impedance spectroscopy for the study of corrosion protection by polymer coatings. *J. Appl. Electrochem.* **1995,** *25*, 187-202.
[34] Scully, J. R. Electrochemical impedance of organic-coated steel: Correlation of impedance parameters with long-term coating deterioration. *J. Electrochem. Soc.* **1989,** *136*(4), 979.

[35] Allahar, K. N.; Bierwagen, G. P.; Gelling, V. J. Understanding AC-DC-AC accelerated test results. *Corros. Sci*. **2010,** *52*(4): 1106-1114.
[36] Latino, M.; Varela, F.; Tan, Y.; Forsyth, M. The effect of ageing on cathodic protection shielding by fusion bonded epoxy coatings. *Prog. Org. Coat.* **2019,** *134*, 58-65.
[37] Inone, P. C.; Garcia, C. M.; Ruvolo-Filho, A. Evaluating barrier properties of organic coatings by water permeation and electrochemical methods. *J. Coat. Technol.* **2003,** *75*(939), 29-36.
[38] Upadhyay, V.; Qi, X.; Wilson, N.; Battocchi, D.; Bierwagen, G.; Forsmark, J.; McCune, R. Electrochemical characterization of coated self-piercing rivets for magnesium applications. *SAE Int. J. Mater. Manuf.* **2016,** *9*(1), 187-199.
[39] Cristoforetti, A.; Rossi, S.; Deflorian, F.; Fedel, M. On the limits of the EIS low-frequency impedance modulus as a tool to describe the protection properties of organic coatings exposed to accelerated aging tests. *Coatings* **2023,** *13*(3): 598.
[40] Kuang, D.; Cheng, Y. F. Effect of alternating current interference on coating disbondment and cathodic protection shielding on pipelines. *Corros. Eng. Sci. Technol.* **2015,** *50*(3), 211-217.
[41] Du, L.; Hu, J.; Duan, M.; Ma, J.; Chen, Z.; Cui, C.; Chen, H.; Qiu, P. Super-impermeable polyurethane coating constructing inspired by passive film structure. *Mater. Today Chem.* **2024,** *42*, 102432.
[42] Zhang, X.; Liu, Y.; Chen, S.; Cheng, X.; Liu, G. The influence of coating defects, cathodic protection and *Pseudomonas aeruginosa* on the corrosion behavior of EH40 steel. *Ocean Eng.* **2025,** *202*, 106108.
[43] Xu, Y.; Ran, J.; Dai, W.; Zhang, W. Investigation of service life prediction models for metallic organic coatings using full-range frequency EIS data. *Metals* **2017,** *7*(7), 274.
[44] Meroufel, A.; Gordon, A.; Thierry, D. Cathodic protection shielding of coated buried pipeline. *J. Coat. Technol. Res.* **2024,** *21*(2), 445-459.
[45] Chen, X.; Su, Y.; Wang, H.; Zhou, Q. Analysis of corrosion behavior and cathodic protection of steel pipeline under alternating current interference. *Coatings* **2025,** *15*(4), 454.